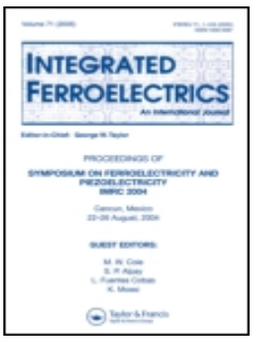

Integrated Ferroelectrics

An International Journal

ISSN: 1058-4587 (Print) 1607-8489 (Online) Journal homepage: https://www.tandfonline.com/loi/ginf20

Relationship between the ferromagnetic phase and the magnetoelectric coupling in hot pressed $Pb(Mg_{1/3}Nb_{2/3})O_3$-$PbTiO_3$ based particulate composites

F. L. Zabotto, Rafael R. G. Paranhos, Menka Jain, A. J. Gualdi, A. J. A. Oliveira, J. A. Eiras & D. Garcia

To cite this article: F. L. Zabotto, Rafael R. G. Paranhos, Menka Jain, A. J. Gualdi, A. J. A. Oliveira, J. A. Eiras & D. Garcia (2016) Relationship between the ferromagnetic phase and the magnetoelectric coupling in hot pressed $Pb(Mg_{1/3}Nb_{2/3})O_3$-$PbTiO_3$ based particulate composites, Integrated Ferroelectrics, 174:1, 121-131, DOI: 10.1080/10584587.2016.1193421

To link to this article: https://doi.org/10.1080/10584587.2016.1193421

Published online: 13 Jul 2016.

INTEGRATED FERROELECTRICS
2016, VOL. 174, 121–131
http://dx.doi.org/10.1080/10584587.2016.1193421

Taylor & Francis
Taylor & Francis Group

Relationship between the ferromagnetic phase and the magnetoelectric coupling in hot pressed $Pb(Mg_{1/3}Nb_{2/3})O_3$-$PbTiO_3$ based particulate composites

F. L. Zabotto[a], Rafael R. G. Paranhos[a], Menka Jain[b], A. J. Gualdi[c], A. J. A. Oliveira[c], J. A. Eiras[a], and D. Garcia[a]

[a]Group of Ferroic Materials, Physics Department, Federal University of São Carlos, São Carlos, SP, Brazil; [b]Department of Physics, University of Connecticut, Storrs, Storrs, CT, USA; [c]Group of Supercondutivity and Magnetism, Physics Department, Federal University of São Carlos, São Carlos, SP, Brazil

ABSTRACT

The influence of ferromagnetic phase properties on the magnetoelectric response of hot pressed particulate composites formed by 80 mol% of $0.675[Pb(Mg_{1/3}Nb_{2/3})O_3]$–$0.325[PbTiO_3]$ as piezoelectric matrix and 20 mol% of $NiFe_2O_4$, $CoFe_2O_4$ or $BaFe_{12}O_{19}$ phases was analyzed. The hot pressing sintering method was suitable for obtaining composites with apparent density higher than 94% and electric resistivity close to 10^9 Ω.m, independently of the ferromagnetic phases used. The magnitude of the magnetoelectric coupling seems to be governed by the piezoelectric properties of ferroelectric PMN-PT matrix, and the zero bias magnetoelectric coefficient values are determined by the ferromagnetic hardness of the magnetic phase.

ARTICLE HISTORY
Accepted 15 January 2016

KEYWORDS
Composite materials; piezoelectricity; piezomagnetism; magnetostriction; magnetoelectric; hot pressing

Introduction

In recent years, magnetoelectric materials (ME), i.e. the materials that show ferroelectric and ferromagnetic ordering simultaneously, have been the focus of research, mainly due to the variety of microstructural phenomena responsible for the coupling between ferroelectric and ferromagnetic orders resulting in the magnetoelectric effect [1,2]. This makes magnetoelectric materials particularly appealing and promising for practical device applications ranging from memory cells [3,4] to new sensitive detection of magnetic field or yet to energy harvesting [5]. The ME effect can be observed in both single-phase and composite materials, and it is characterized by an induction of magnetization when the material is under an electric field, or an induction of electric polarization resulting from the application of a magnetic field. In the case of single-phase magnetoelectric materials, the effect is observed only at low temperatures and the achievable magnitude of the ME signals is not sufficient for practical applications [1,4–6]. On the other hand, in composite materials using the concept of product properties introduced by Van Suchtelen [1,5], the ME

CONTACT F. L. Zabotto zabotto@df.ufscar.br

effect is understood as an interaction between piezoelectric and magnetostrictive (or piezomagnetic) constituent phases through mechanical coupling [1,7]. Particularly, for 0–3 connectivity ceramic composites, the inherent key points to achieve the ME effect can be summarized as: 1) individual phases should be in equilibrium; 2) no mismatch between grains should be present; 3) the magnitude of the magnetostrictive/piezoelectric coefficients of magnetostrictive and piezoelectric phases should be high; and 4) electrical resistivity of the magnetic phase should be high enough to avoid leakage during electric poling [1,7]. According to these considerations, a suitable combination of magnetostrictive/piezomagnetic and piezoelectric phases can yield a strong ME response, which depends on the choice and distribution of the constituent phases. Most 0–3 connectivity composite materials, or particulate composites, use Pb (Zr,Ti) O_3 (or PZT) as piezoelectric phase and ferrite or hexaferrite-based compounds as ferromagnetic phase [5,7]. PZT ferroelectric ceramics present relatively higher piezoeletrics coefficients than other ferroleletric materials [8]. Several studies have reported a good chemical stability of PZT with nickel ferrites, which results in a high magnetoelectric coupling [7]. On the other hand, when cobalt ferrite, which has higher magnetostrictive coefficients, is used in the PZT matrix, results show a reduced ME coefficient [8]. Nevertheless, due to differences in the processing conditions of the piezoelectric and magnetic phases, it is rather difficult to find the ideal sintering conditions to obtain optimum-quality magnetoelectric composites for technological applications. There are other ferroelectric materials that show high piezoelectric coefficient, such as Pb $(Mg_{1/3}Nb_{2/3})O_3$-$PbTiO_3$ (PMN-PT) which is a good candidate for replacing PZT [9]. Magnetoelectric composites using PMN-PT as a piezoelectric phase in the 2–2 connectivity pattern have shown interesting ME response [9]. The small number of studies available on the 0–3 particulate composites mainly discuss the effect of the ferromagnetic phase on the properties of PMN-PT particulate composites. Considering that, this paper investigates the influence of the various ferromagnetic spinel structured ferrites (like $CoFe_2O_4$ and $NiFe_2O_4$) and the hexagonal structured ($BaFe_{12}O_{19}$) phase on the ME response of the 0–3 particulate composites using the PMN-PT as matrix. The hot pressing sintering method was used in this study in order to achieve high density samples. The technique used also reduced the sintering temperature as compared to the temperature used in the conventional sintering process.

Experimental procedure

Magnetoelectric composites of compositions (80 mol%) [0.675(Pb $(Mg_{1/3}Nb_{2/3})O_3$ – $0.325PbTiO_3$] (or PMN-PT) and (20 mol%) ferrite ($NiFe_2O_4$ (NFO), $CoFe_2O_4$ (CFO) and $BaFe_{12}O_{19}$(BaM)) were prepared by the conventional solid state reaction method. The cobalt and the nickel ferrite ceramic powders were prepared by using Co_3O_4, NiO and Fe_2O_3 as starting materials. The powders were mixed through ball-milling (distilled water with ZrO_2 cylinders), calcined at 900°C for 4 h and then ball-milled again (for grinding) during 10 h. The BaM powder was prepared by mixing BaO and α-Fe_2O_3 at an Fe/Ba ratio of 12, ball milling at 200 rpm for 2 h

and finally calcining at 1200°C/ 4 h. The PMN-PT ceramic powder was obtained through the columbite method. The columbite precursor, $MgNbO_6$, was prepared with MgO and Nb_2O_5 reagent powders, and calcined at 1100°C for 4 h. After that, following the batching formula $0.675(Pb(Mg_{1/3}Nb_{2/3})O_3 - 0.325PbTiO_3$, the magnesium niobate was mixed with PbO and TiO_2, calcined at 900°C for 4 h and ball milled for 10 h. The particulate composites were prepared by mixing (again through ball-milling) the ferrite and the ferroelectric phase in a 20/80 molar ratio. The powders were then uniaxially and isostatically cold-pressed into pellets (∼10 mm in diameter and ∼10 mm thick). The specimens were densified in oxygen by uniaxial hot pressing, under a maximal pressure of 12 MPa using a Thermal Inc. HP22-0614-SC hot uniaxial press. For PMN-PT/NFO and CFO pellets, the selected temperature condition was 1050°C for 0.5 h. On the other hand, for PMN-PT/BaM this condition was reduced to 1000°C/0.5 h.

The phase identification of the fired specimens was performed through X-ray diffraction (XRD) analysis using a Rigaku Rotaflex RU200B powder diffractometer, with CuK_α radiation 2θ from 20° to 60° and 2°/min of step. The apparent density (ρ_{app}) was obtained by a method based on Archimedes principle, with distilled water as immersion liquid. Dielectric characterization was performed on the ceramics with gold sputtered surfaces and using a HP 4194A Impedance Gain Phase Analyzer, over a temperature range of $30°C < T < 400°C$, at a constant rate of 2°C/min, for a frequency range of 100 Hz to 1 MHz. For NFO and CFO composites the magnetization measurements were made using a magnetometer extraction of Physical Properties Measurement System (PPMS) model 6000 Quantum Design, at room temperature (300 K) and a magnetic field up to 50 kOe. These composites were poled under the same condition, at electric bias field of 20 $kVcm^{-1}$ for 30 min, at room temperature. On the other hand, magnetic measurements in BaM composite were carried out using a magnetic field up to 15 kOe, in a VSM attached to the PPMS system. Additionally, poling condition was changed to 15 $kVcm^{-1}$ for 30 min, due to concerns of electric breakdown. Ferroelectric loops for polarization versus electric field were taken through a Sawer-Tower circuit. For magnetostrictive measurements, capacitive cells using a model 2550A Andeen-Hagerling capacitance bridge were used. The magnetoelectric voltage coefficient α_{33} were determined by measuring the magnetic field induced voltage across the composite, using a lock-in amplifier with DC bias magnetic field up to 8 kOe, overlapped by an ac magnetic field (5 Oe at 1 kHz).

Results and discussion

The XRD patterns of PMN-PT/ferrites ME composites are shown in figure 1. The diffraction patterns show the presence of the ferrite cubic spinel structure and hexagonal structure for ferromagnetic phases and the PMN-PT tetragonal perovskite structure for ferroelectric phases without traces of residual phases. An analysis of the changes in the *c/a* ratio of the matrix and *a* lattice parameter of the CFO and NFO phases can be seen in the table 1. It shows the similar values of *c/a* ratio for PMN-PT

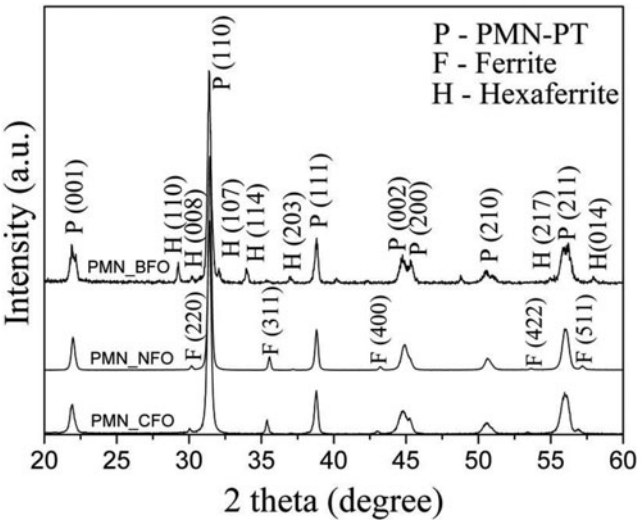

Figure 1. XRD patterns of the PMN-PT/CFO, PMN-PT/NFO and PMN-PT/BaM hot pressed composites at 1050°C and 1000°C for 0.5h, under pressure of 12 MPa, in oxygen atmosphere, respectively. The peak identification is related to the JCPDS files # 22–1086 (CFO), #39–1007 (PMN-PT) and #44–1485 (NFO).

and for the composites PMN-PT/ferrites. The *a* lattice parameter of the CFO and NFO phases in the composites remains constant close to 8.40 and 8.37 Å, respectively. The difference between *a* lattice parameter of the CFO and NFO is related to the different size of the Ni^{+2} ions (0.69 Å) compared to the Co^{+2} ions (0.72 Å) present in the NFO and CFO phases, respectively. A similar behavior is noticed in the PMN-PT/BaM composites (table 1), and the lattice parameters remain constant in the BaM and PMN-PT/BaM phases. The invariance of the c/a ratio of PMN-PT matrix and lattice parameter of the ferromagnetic phases suggest that chemical reaction has not significantly occurred between the ferroelectric and ferrite phases during the hot pressing process, at the measurement resolution. The apparent density analyses of the composites confirm that both composites exhibit high density (values reached 95%).

High electrical resistivity ($\sim 10^9$ Ωcm), measured with a model 617 Keithley multimeter, was achieved for all cases, which can be explained based on the addictive behavior between the electrical properties of PMN-PT (electrical resistivity of $\sim 10^{12}$

Table 1. Lattice parameter, relative density and electric resistivity values for PMN-PT, CFO and NFO phases, PMNPT/CFO and PMN-PT/NFO particulate composites.

	c/a ratio	Lattice parameter (Å)	Relative density (%)	Electric resistivity (Ω.cm)
PMN-PT	1.005 ± 0.002	—	97.3 ± 0.2	$(7 \pm 2) \times 10^{12}$
CFO	—	8.40 ± 0.03	96.7 ± 0.2	$(8 \pm 3) \times 10^{6}$
NFO	—	8.35 ± 0.02	95.4 ± 0.4	$(2.2 \pm 0.3) \times 10^{6}$
BaM	3.935 ± 0.002	$a = 5.88 \pm 0.02$ $c = 23.12 \pm 0.02$	97.0 ± 0.2	$(2.6 \pm 0.3) \times 10^{9}$
PMN-PT/CFO	1.006 ± 0.002	8.40 ± 0.02	97.8 ± 0.1	$(6 \pm 1) \times 10^{9}$
PMN-PT/NFO	1.003 ± 0.002	8.37 ± 0.04	97.1 ± 0.2	$(1.7 \pm 0.2) \times 10^{9}$
PMN-PT/BaM	1.003 ± 0.002	$a = 5.88 \pm 0.02$ $c = 23.13 \pm 0.02$	94.0 ± 0.5	$(3 \pm 1) \times 10^{10}$

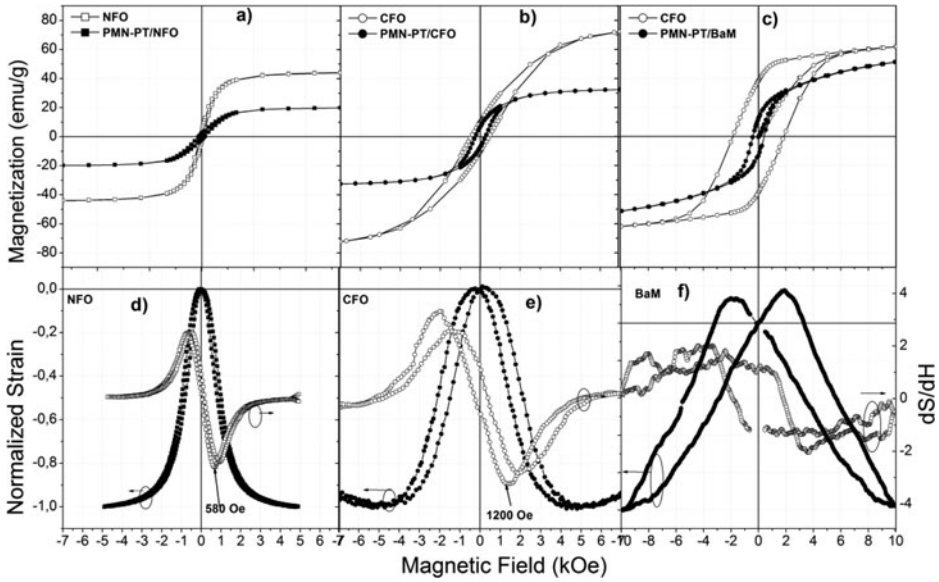

Figure 2. Room temperature magnetization as a function of applied magnetic field for: a) PMN-PT/NFO composite and NFO ceramic; b) PMN-PT/CFO composite and CFO ceramic; c) PMNPT/BaM and BaM ceramic; and room temperature strain as a function of applied magnetic field for: d) NFO; e) CFO; and f) BaM ceramics.

Ωcm) and those of the ferromagnetic phases (electrical resistivity of $\sim 10^6$ Ωcm). It means that the adopted processing protocol was suitable to obtain composites with good microstructure and electrical properties, regardless of the magnetic phase of the compounds.

Figure 2a shows the room temperature magnetic hysteresis loops for PMN-PT/NFO composites and NFO ceramics. The saturation magnetization of the NFO ferrite is larger than that of the PMN-PT/NFO composite: 44 emu/g and 20 emu/g, respectively. Figure 2b shows the magnetization results for the f PMN-PT/CFO composites and CFO ceramics. The saturation magnetization of the ferrite is larger than that of the composite: 76 emu/g and 33 emu/g, respectively. Similarly, in figure 2c, a reduction of saturation magnetization can be observed for the PMN-PT/BaM composite when compared with the BaM phase from 66 emu/g to 45 emu/g. In addition, it can be observed that the magnetic field used (up to 10 kOe) is not sufficient to reach the saturation conditions. In all cases, the composites present a typical ferromagnetic response, with the coercive magnetic field (H_c) increasing from 75 Oe and 270 Oe to 500 Oe, and remanent magnetization (M_r) from 2 emu/g to 20 emu/g for PMN-PT/NFO, PMN-PT/CFO and PMN-PT/BaM, respectively. This increment in the Hc and Ms values is a consequence of the hardness ferromagnetic behavior typical of cobalt ferrites and Barium hexaferrites. A decrease in the saturated magnetization and remnant magnetization observed in composites, in comparison with those of the ferrite phases, is related to the dispersion of the magnetic phase in a non-magnetic phase (the PMN-PT one), which decreases the interaction between the magnetic particles. From these results, it could be inferred that the magnetic

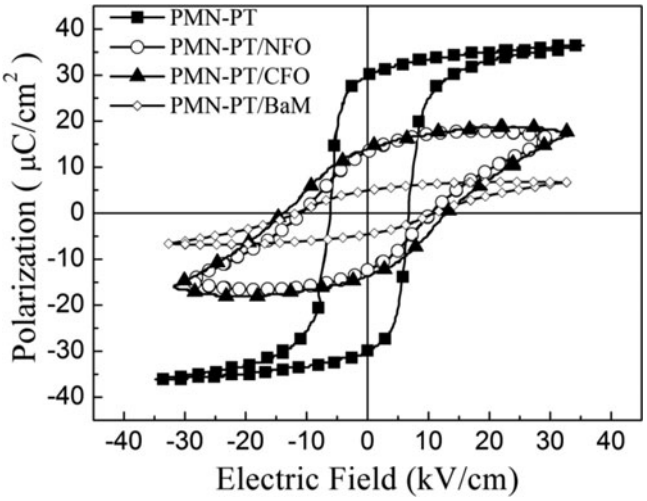

Figure 3. Ferroelectric hysteresis loops of the PMN-PT ceramics and related magnetoelectric composites with NFO, CFO and BaM phases.

properties of these composites are governed by a vector sum of all the individual ferrite contributions, since the ferroelectric PMN-PT is a diamagnetic phase (not shown here).

Figures 2d, 2e and 2f show the relative strain curve as a function of the magnetic field for NFO, CFO and BaM phases, respectively. It is clear that the magnetic field in which the maximum strain variation occurs depends on the ferrite phase (NFO and CFO phases). The derivative of the magnetostrictive strain (dS/dH) shows that the maximum variations of strain are close to 580 Oe and 1200 Oe for NFO and CFO ferrites, respectively. In agreement with the magnetization results, the shifts of the maximum dS/dH towards higher fields for CFO ferrite samples are a consequence of the high magnetic anisotropy of the CFO phase, in comparison with the NFO ferrite phase. In the case of BaM, we have not observed a peak in the field derivative of strain (dS/dH). A hysteresis curve for the variation of strain with magnetic field is noticeable in figure 2f, and it is related to the hard ferromagnetic nature of BaM resulting in a piezomagnetic contribution to the strain, in contrast with the NFO or CFO phases.

Figure 3 shows the hysteresis loops of the polarization versus electrical field for the PMN-PT ceramics and related composites with NFO, CFO and BaM phases. It can be observed that the ferroelectric behavior of composites is practically independent of the type of the ferrite phase in the composites. There is a suppression of the polarization (from 35 μC/cm^2 to $\sim$17 μC/cm^2) due to the presence of a non-ferroelectric phase, i.e. the ferrite phase. Such material with low dielectric permittivity ($\varepsilon'_{\text{ferrite}} \sim 100$) dilutes the electrical susceptibility of the ferroelectric matrix ($\varepsilon'_{\text{PMN-PT}} \sim 2000$). Added to this fact, it is observed that the suppression of ferroelectric behavior is larger for the PMN-PT/BaM composite, which shows low apparent density ($\sim$94%) due to the presence of porosity, further increasing the degree of non-ferroelectric phase in the composite. Also, there is an increase in the coercive

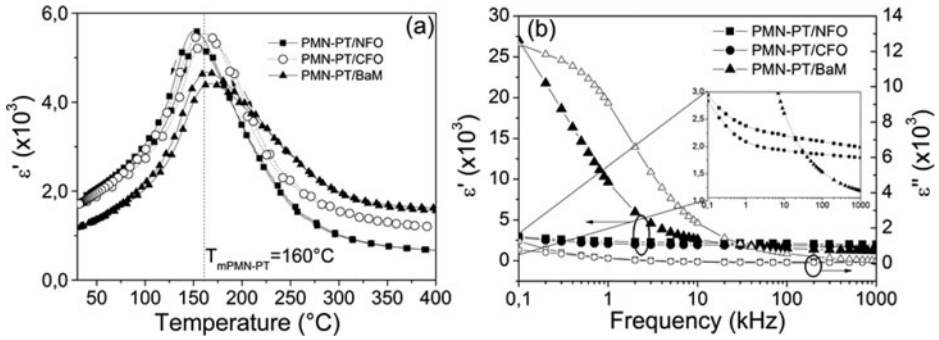

Figure 4. (a) Real part of electric permittivity (ε') at 1MHz, and (b) frequency dependence of ε' and ε'', for PMN-PT/NFO, PMN-PT/CFO and PMN-PT/BaM composites.

fields of the composites compared to that of the pure PMN-PT phase, which can be related to the decrease in the electrical resistivity when the semi-conductive ferrite phases are added to the ferroelectric matrix.

The real part of the dielectric permittivity, ε', as a function of temperature for the composites is shown in figure 4a. The dielectric permittivity increases with temperature up to ~160°C for all composites. Above these temperatures, ε' decreases slowly, indicating maximum ε' values at these temperatures, or T_{max}. PMN ferroelectric ceramics with 32.5 mol% of PT have a structural transition from cubic to tetragonal symmetry, i.e. from paraelectric to ferroelectric phase transition at 160°C [10]. Thus, it can be inferred that the maximum ε'values observed for all composite compounds could be related to the paraelectric-ferroelectric transition of the PMN-PT matrix. At 1MHz, the maximum values of ε' are close to 5600 for PMN-PT/NFO and PMN-PT/CFO and 4200 for PMN-PT/BaM. Lower ε' values for the composites, compared to those of the pure PMN-PT matrix (ε'_{max} ~25000) are expected because the dielectric properties of composites can be represented by combined properties of the constituent phases generally governed by logarithm mix rules. In addition, the maximum value of ε' is generally influenced by extrinsic factors such as porosity or stress, which affect the dielectric properties of ceramics [11]. Additionally, the reduced grain size of the ferroelectric phase generates internal stress, resulting in a reduction in the domains movement, diminishing the dielectric properties of dielectrics [12]. In our results, it is possible to see an increase of porosity in PMN-PT/BaM composites compared to the NFO and CFO composites, which can be responsible for the reduction of ε' in PMN-PT/BaM composites. On the other hand, it is interesting to note the unchanged values of T_{max} in the PMN-PT/CFO and PMN-PT/BaM composites. Such results are indicative of the fact that the PMN-PT and ferrite phases remained in the unreacted phase form (as confirmed by the XRD analyses). On the other hand, a lower T_{max} for the PMN-PT/NFO composite can be the result of inter-diffusion between the NFO and PMN-PT phases.

The plots of the dielectric permittivity (real ε', and imaginary part ε") with frequency at room temperature for all composites are shown in figure 4b. It has been found that ε' and ε" decrease steeply at low frequencies and remain constant

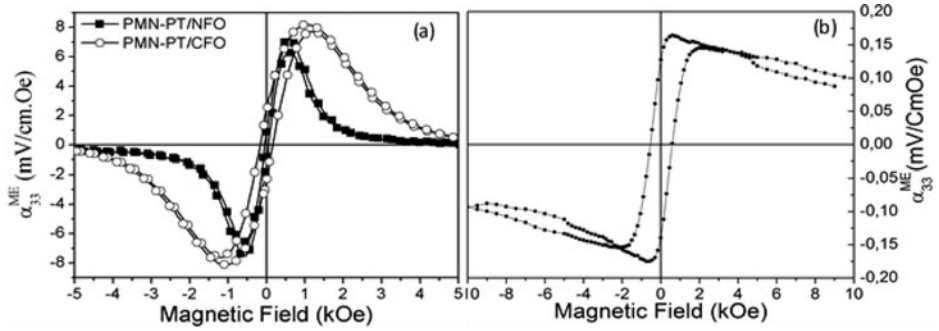

Figure 5. Magnetoelectric coefficient as a function of applied magnetic field for (a) PMN-PT/NFO and PMN-PT/CFO composites; and (b) PMN-PT/BaM composites.

at high frequencies, indicating that the dielectric dispersion is independent of the ferromagnetic phase in the composites. Generally, in ferrite composites, high values of dielectric permittivity at low frequencies are associated to the electrical contribution from the chemical heterogeneity of the materials and/or also due to the existence of both valence iron states, Fe^{3+} and Fe^{2+} [13]. The rotational displacement of the $Fe^{3+} \leftrightarrow Fe^{2+}$ dipoles results in orientation polarization, in which case the net magnitude decreases with frequency [14, 15]. Under alternating electric field over 10^4 Hz, the extrinsic contribution to the polarization evanesces and the dipolar ferroelectric contribution is dominant.

Figure 5a shows the magnetic field dependence of the ME coefficient, $\alpha^{ME}{}_{33}$, for the PMN-PT/NFO and PMN-PT/CFO composites. As observed, the ME coefficient increases up to 7.2 mV/cm.Oe at 570 Oe DC bias field and up to 8.5 mV/cm.Oe at 1200 Oe dc bias field for PMN-PT/CFO, which is comparable to the other investigated composites [13–18]. Nevertheless, it is lower than the Ni-ferrite/PZT [5, 7] composites obtained by conventional sintering. In the latter case, the ME coefficient values were found to be strongly dependent on the grain size distribution. In spite of the enhancement of the microstructure quality and electrical properties obtained through the hot pressing method, our lower ME values compared to those of the refs. 5 and 7 may be associated to the small average grain size ($\sim 0.6 \mu$m) obtained through this method, compared to that of the conventional sintering (larger than 1μm). In fact, the ME response intensifies as the grain size increases, due to the enhancement of the piezoelectric properties [19].

In the case of PMN-PT/NFO and PMN-PT/CFO, the shape of the magnetoelectric voltage curve (similar in both cases) follows the magnetostrictive behavior of each magnetic phase (Figure 2 d and 2 e). The magnetic field in which the $\alpha^{ME}{}_{33}$ values are maximum occurs close to ~570 Oe and ~1100 Oe, for PMN-PT/NFO and PMN-PT/CFO respectively. These values are in agreement with the magnetic field region where the maximum variations of strain occur for the NFO and the CFO phases (~580 Oe and ~1200 Oe, respectively). Also, it can be seen that the PMN-PT/CFO composite shows a more evident hysteretic loop in the ME response when compared to the magnetoelectric curve of PMN-PT/NFO composites. Figure 5b shows the magnetoelectric curve for PMN-PT/BaM composites. It is important to

observe the shape of a hysteresis behavior curve without a pronounced maximum of $\alpha^{ME}{}_{33}$ values. This same hysteretic behavior was observed in the magnetoelectric composites of the $BaTiO_3/BaFe_{12}O_{19}$ system 0020/20. This suggests that the hysteric behavior is due to the piezomagnetic behavior, which could be correlated with the high magnetic anisotropy inherent to the BaM phase 0021/21. In the case of PMNPT/BaM, it is possible to switch the $\alpha^{ME}{}_{33}$ coefficient from +0.16 mV/cm.Oe to – 0.16 mV/cm.Oe by switching the magnetic field. These values are comparable with BT/BaM system found in literature reports [22, 23]. In this case, the maximum α_{33} values remain at zero bias field, indicating a remnant behavior. This memory effect in α_{33} value is clearly related to the dS/dH curves, which show a piezomagnetic curve shape in comparison with the magnetostrictive behavior observed for NFO and CFO phases (figure 2 d and 2e). However, the maximum $\alpha^{ME}{}_{33}$ values decrease in the PMN-PT/BaM phase, in comparison to PMN-PT/NFO and PMN-PT/CFO, which can be related to the low apparent density values obtained that affect the mechanical coupling between phases. Similar values of $\alpha^{ME}{}_{33}$, regardless of the ferrite phase used (NFO or CFO) indicate that the magnitude of the magnetoelectric coupling appears to be governed by the piezoelectric properties of the ferroelectric PMN-PT matrix, as expected. On the other hand, the zero bias magnetoelectric coefficient values are determined by the ferromagnetic hardness of ferromagnetic phase, which enhances the primary mechanical coupling (piezomagnetic effect) than the secondary mechanical coupling (magnetostrictive effect).

Conclusions

In summary, the influence of the ferromagnetic behavior of the ferrite phase on the ME response of (80 mol%)$Pb(Mg_{1/3}Nb_{2/3})_{0.68}Ti_{0.32}O_3$ +(20 mol%) $CoFe_2O_4$, $NiFe_2O_4$ or BaM particulate composites densified by uniaxial hot pressing was investigated through the structural, microstructural, dielectric, magnetic, magnetostrictive and magnetoelectric properties. It was seen that the magnetic properties of the composites are determined by the magnetic characteristic of the ferrite phase diluted in a nonmagnetic matrix. Thus, the dielectric properties of these composites are governed by combined properties, in which the ferroelectric phase is an active and mainly responsible player. The ME response in all composites has been attributed to the mechanically mediated effect, in which the ME values are strongly dependent on the change of magnetic induced strain. The magnitude of the magnetoelectric coupling seems to be governed by the piezoelectric properties of ferroelectric PMN-PT matrix, and the zero bias magnetoelectric coefficient values are determined by the ferromagnetic hardness of the ferromagnetic phase. The zero bias magnetoelectric effect was enhanced for BaM composites that shows a first order mechanical coupling (piezomagnetic effect) in comparison to the CFO and NFO composites that shows a second order mechanical coupling (magnetostrictive effect). In the case of PMNPT/BaM, it was possible to switch the $\alpha^{ME}{}_{33}$ coefficient from +0.16 mV/cm.Oe to – 0.16 mV/cm.Oe by switching the magnetic field, which indicates a memory behavior.

Acknowledgments

The authors thank Mr. Francisco José Picon and Mrs. Natália Aparecida Zanardi for the technical support, Prof. Yvonne P. Mascarenhas (Crystallography Group of the Physics Institute of USP-São Carlos) for the use of the XRD Lab facilities, and FAPESP ((Proc. 2008/04025-0 and 2010/07518-7), CAPES (proc. 3012/2014) and CNPq (proc. 477354/2013-0) for the financial support.

References

1. C. W. Nan et al. Multiferroic magnetoelectric composites: Historical perspective, status and future Directions. *J. Appl. Phys.* 208; **103**, 031101.
2. C. Ederer, N. A. Spaldin Magnetoelectrics – A new route to magnetic ferroelectrics. *Nature Materials* **3**, 849–851 (2004).
3. M. Bibes, A. Barthélémy Multiferroics: Towards a Magnetoelectric Memory. *Nature Materials* **7**, 425–426 (2008).
4. J. Scott Data Storage: Multiferroic Memories. *Nature Materials*. **6**, 256–257 (2007).
5. R. A. Islam, S. Priya Progress in Dual (Piezoelectric-Magnetostrictive) Phase Magnetoelectric Sintered Composites. *Adv. Cond. Matter Phys.* **2012**, 320612 (2012).
6. N. A. Hill Why are there so few magnetic ferroelectrics? *J. Phys. Chem. B.* **104**, 6694–6709 (2000).
7. J. Ryu, et al. Magnetoelectric Effect in Composites of Magnetostrictive and Piezoelectric Materials. *J. Electroceram.* **8**, 107–119 (2002).
8. G. Sreenivasulu, H. Qu, G. Srinivasan Multiferroic Oxide Composites: Synthesis, Characterisation and Applications. *Mat. Sci. and Tech.* **30**(13a), 1625–1632 (2014).
9. G. H. Haertling Ferroelectric ceramics: History and Technology. *J. Am. Ceram. Soc.* **82**, 797–818 (1999).
10. M. H. Lente, et al. Effect of the Composition and Sintering Process on the Electrical Properties in $Pb(Mg_{1/3}Nb_{2/3})O_3$-$PbTiO_3$ Ceramics. *J. Eur. Ceram. Soc.* **24**, 1529–1533 (2002).
11. W. Cai, et al. Effects of Grain Size on Domain Structure and Ferroelectric Properties of Barium Zirconate Titanate Ceramics. *J. Alloy Compd.* **480**, 870–873 (2009).
12. W. Jo, et al. Effects of Grain Size on the Dielectric Properties of $Pb(Mg_{1/3}Nb_{2/3})O_3$-30 mol% $PbTiO_3$ Ceramics. *J. Appl. Phys.* **102**, 074116 (2007).
13. B. K. Bammannavar, L. R. Naik, B. K. Chougule Studies on Dielectric and Magnetic Properties of $(x)Ni_{0.2}Co_{0.8}Fe_2O_4$+(1-x) Barium Lead Zirconate Titanate Magnetoelectric Composites. *J. Appl. Phys.* **104**, 064123 (2008).
14. V. L. Mathe, A. D. Sheikh, A. Fawzi Microstructure-property Relationship in Magnetoelectric Bulk Composites. *J. Magn. Mag. Mater.* **323**, 740–747 (2011).
15. B. K. Chougule, et al. Synthesis and Magnetoelectric Properties of $y(Ni_{0.3}Cu_{0.4}Zn_{0.3}Fe_2O_4)$ + (1-y)[50%$BaTiO_3$+50%PZT] ME composites. *J. Alloys Compd.* **490**, 195–199 (2010).
16. L. M. Hrib, O. F. Caltun Effects of the Chemical Composition of the Magnetostrictive Phase on the Dielectric and Magnetoelectric Properties of Cobalt Ferrite-Barium Titanate Composites. *J. Alloys Compd.* **509**, 6644–6648 (2011).
17. A. D. Sheikh, V. L. Mathe Effect of the Piezomagnetic NiFe(2)O(4) Phase on the Piezoelectric $Pb(Mg_{1/3}Nb_{2/3})0.67Ti_{0.33}O_3$ Phase in Magnetoelectric Composites. *Smart Mater. Struct.* **18**(6), 065014–19 (2009).
18. Z. J. Shen, et al. Magnetoelectric Composites of Nickel Ferrite and Lead Zirconate Titanate Prepared by Spark Plasma Sintering. *J. Eur. Ceram. Soc.* **27**, 279–284 (2007).
19. S. Priya, R. A. Islam Effect of Piezoelectric Grain Size on Magnetoelectric Coefficient of $Pb(Zr_{0.52}Ti_{0.48})O_3$-$Ni_{0.8}Zn_{0.2}Fe_2O_4$ Particulate Composites. *J. Mater. Sci.* **43**, 3560–3568 (2008).

20. J D S Guerra, et al. Multiferroism and Magnetoelectric Coupling in $(PbZr_{0.65}Ti_{0.35}O_3)0.97$-$(BaFe_{12}O_{19})0.03$ Ceramic Composite. *J. Appl. Phys.* **114**(22), 224113 (2013).
21. A. Srinivas, R. Gopalan, V. Chandrasekharan Room Temperature Multiferroism and Magnetoeletric Coupling in $BaTiO_3$-$BaFe_{12}O_{19}$ System. *Solid State Comm*. **149**, 367–370 (2009).
22. D. V. Karpinsky, et al. Local Probing of Magnetoelectric Coupling in Multiferroic Composite of $BaFe_{12}O_{19}$-$BaTiO_3$. *J. Appl. Phys.* **108**, 042012 (2010).
23. A. Srinivas, et al. Improved Magnetoelectricity by Uniaxial Magnetic Field Pressed and Sintered Composites in $BaTiO_3$(x)-$BaFe_{12}O_{19}$(1-x) System (x= 0.8, 0.6). *Mat. Sci. Eng. B.* **8**, 289–293 (2010).